

Room-temperature hydrogenation of levulinic acid by uniform nano-TiO₂ supported Ru catalysts

Guoqiang Li^{a,b}, Huanhuan Yang^{a,b}, Mei Cheng^{a,b}, Wei Hu^{a,b}, Lihong Tian^{a,b}, Wuxiang Mao^{c,**}, Renfeng Nie^{a,b,*}

^a Hubei Collaborative Innovation Center for Advanced Organic Chemical Materials, Hubei University, Wuhan 430062, PR China

^b Ministry-of-Education Key Laboratory for the Synthesis and Application of Organic Functional Molecules, School of Chemistry and Chemical Engineering, Hubei University, Wuhan 430062, PR China

^c Hubei Collaborative Innovation Center for Green Transformation of Bio-resources, College of Life Sciences, Hubei University, Wuhan, Hubei 430062, PR China

ARTICLE INFO

Keywords:

TiO₂ nanoparticles
Electron donation
Room-temperature hydrogenation
Biomass
Water

ABSTRACT

Uniform TiO₂ nanoparticles (NPs) is synthesized by a facile hydrothermal approach and used as support for Ru NPs. It is found that HF amount has a considerable influence in the size and uniformity of TiO₂ NPs, and the optimized Ru/TiO₂-0.4 is highly efficient for fast room-temperature hydrogenation of levulinic acid (LA) to γ -valerolactone (GVL) in water. For example, Ru/TiO₂-0.4 Exhibits 5.1 times higher activity in comparison with commercial TiO₂ supported Ru (Ru/TiO₂-C), and affords 97.4% LA conversion and > 99% GLV selectivity at 30 °C and 1 MPa H₂ for 30 min. In particular, Ru/TiO₂-0.4 can even reach 88.5% LA conversion at lower temperature to 10 °C. This catalyst is stable for recycle and also affords good conversion as well as high selectivity for hydrodeoxygenation (HDO) of biomass-derived vanillin, attributed to smaller sized TiO₂ NPs, easier electron donation from TiO₂ to Ru and higher reducibility of Ru species.

1. Introduction

The use of renewable biomass to replace limited fossil fuels has been recognized as a potential solution for the sustainable production of liquid fuels and valuable chemicals [1]. Biomass can be converted to bulk products through bio-refinery process [2]. Among them, levulinic acid (LA) is one of these promising platform molecules, as it can be transformed to a variety of derivatives, such as fuel additives, monomer of polymers and other high value-added chemicals [3]. Downstream processing of LA actually involve one of versatile molecules- γ -valerolactone (GVL), making the hydrogenation of LA to GVL a reaction of immense importance [4].

In the last several years, many metal-based catalysts, including non-noble metal (Cu, Ni, and Co)-supported and noble metal (Pt, Pd, and Ru)-supported catalysts, have been reported for LA hydrogenation [4–17]. However, harsh reaction conditions (150–300 °C, 3–7 MPa H₂) are required to obtain a high GVL yield over non-noble catalysts [5,7,9,10]. Furthermore, the metal leaching for these catalysts due to their low tolerance to the highly polar and acidic environment, leads to the easy deactivation of catalysts [9,11]. Among noble metal catalysts, Ru-based catalysts generally give the highest GVL productivities, with

Ru/C being highly active and selective for hydrogenation of LA [16,18,19]. The optimal temperature windows for LA hydrogenation are above 70 °C, which leave sample room for improvements [4,20]. While carbon supports are stable under the highly polar and acidic conditions of a LA hydrogenation process, they do not survive the multiple regeneration cycles required for catalyst reactivation by burning off coke at high temperatures [21].

Low-temperature efficient catalysts for LA hydrogenation, especially those operating at room temperature, are of interest for industrial application, because it is more energy saving and produces minimized humins and/or C–C cracking byproducts [22]. More importantly, because of the acidity and high polarity of LA, low temperature would be beneficial for relieving leaching and deactivation of metal sites, endowing catalysts with long life [18].

In order to achieve high LA hydrogenation activity at low temperature, the morphology and the inner properties (such as charge transfer, acid-base, reducibility, hydrogen spillover, metal-support interactions, etc.) of the support material have been shown to be the descriptors that govern their catalytic properties [22–26]. Because of the high dispersion in medium and low diffusion resistance towards substrates, nanosized supports are of superiority for metal-mediated

* Corresponding author at: Hubei Collaborative Innovation Center for Advanced Organic Chemical Materials, Hubei University, Wuhan 430062, PR China.

** Corresponding author.

E-mail addresses: maowuxiang@163.com (W. Mao), refnienie@163.com (R. Nie).

low-temperature hydrogenation [27,28]. For example, both Huang and Li reported that two-dimensional structure of graphene is active for Ru-catalyzed room-temperature hydrogenation of LA into GLV at high hydrogen pressure (4 MPa), in which the electron transfer between Ru⁰ and RGO leads to the formation of an electron-rich state of Ru⁰ NPs that are highly effective for activating C=O bonds [14,22,29]. Although oxidation-exfoliation method is commonly adopted for preparing graphene [30], the tedious, high-cost, non-environmentally friendly process makes it after all less suitable for industrial use.

Herein, we synthesized uniform TiO₂ NPs with a size of 35 nm via a facile hydrothermal method. After loading Ru by impregnation method, this catalyst (Ru/TiO₂) displayed a superior room-temperature and low-hydrogen-pressure (≤ 1 MPa) activity and high stability in the aqueous hydrogenation of LA to GVL. The influence of the HF amount on the textural structure of TiO₂ and the catalytic performances of Ru/TiO₂ are investigated. We also discuss the catalytic performance of Ru catalysts under different reaction conditions such as variation in pressure, solvent and amount of catalyst on the hydrogenation of FA at room temperature. This work may promote the investigation of low-temperature hydrogenation of biomass in the chemical industry.

2. Experimental section

2.1. Materials

The used chemicals included tetra-butyl orthotitanate (TBOT, 98%, Feida), RuCl₃ (Ru = 45–55%, Sinopharm), hydrofluoric acid (HF, 40%, Sinopharm). All other chemicals were of analytical purity if not otherwise noted.

2.2. Preparation of nano-TiO₂

In a typical synthesis for nano-TiO₂, 9.96 g of TBOT was added dropwise into a Teflon-lined stainless steel autoclave containing different amounts (0.4 mL, 1 mL, 2 mL and 3 mL) of HF under magnetic stirring. The autoclave was kept at 200 °C for 24 h in an electric oven, then cool down naturally to room temperature. The anatase TiO₂ samples were harvested by centrifugation, washed thoroughly with deionized water 3 times and absolute ethanol 2 times, and then dried in vacuum at 60 °C overnight. The as-synthesized sample was calcined at 400 °C for 4 h in air at a heating rate of 5 °C/min. The as-prepared TiO₂ samples were denoted as TiO₂-0.4, TiO₂-1, TiO₂-2 and TiO₂-3, in which the volume of HF used is 0.4 mL, 1 mL, 2 mL and 3 mL respectively.

2.3. Preparation of Ru/nano-TiO₂

One gram of the support was dispersed in water (50 mL), and then added with a certain amount of metal salts while stirring. After 5 min under ultrasound, the water was removed by reduced pressure at 60 °C. The resulting powder heated to 250 °C at a rate of 5 °C/min under a flow of hydrogen and kept for 2 h. The resulting Ru catalyst was named as Ru/TiO₂-x. As reference, commercial TiO₂ was also used as support for Ru, the resulting sample was named as Ru/TiO₂-C. The real amount of Ru loading was detected via inductively coupled plasma-atomic emission spectroscopy (ICP, Plasma-Spec-II spectrometer). About 5 mg catalysts were digested using 20% aqua regia, and all the particles in the solution were removed before the analysis.

2.4. Characterization

Powder X-ray diffraction (XRD) was performed on a Bruker D8A25 diffractometer with CuK α radiation ($\lambda = 1.54184$ Å) operating at 30 kV and 25 mA. N₂ adsorption was carried out at -196 °C using an auto-adsorption analyzer (Micromeritics, TriStar II). Scanning electron images (SEM) were collected on JEOL (JSM6700F) at an accelerating voltage of 15 kV. Transmission electron microscope (TEM) images were

obtained using an accelerating voltage of 200 kV on a JEOL-135 2010F Transmission Electron Microscope. X-ray photoelectron spectra (XPS) were recorded on a Perkin-Elmer PHI ESCA system.

TPR experiments were performed in a flow setup using 20 vol% H₂ in N₂ at a flow rate of 50 mL/min. The TPR of the calcined Ru/TiO₂-x samples was performed from room temperature to 400 °C at a heating rate of 5 °C/min. A thermal conductivity detector (TCD) was used to monitor the H₂ consumption. Before starting the TPR procedure, the sample was pretreated at 200 °C for 30 min in the N₂ flow of 100 mL/min and then cooled down to room temperature.

2.5. Catalytic tests

The hydrogenation reaction was carried out in a 25 mL stainless autoclave with a Teflon liner. In a typical procedure, a certain amount of catalyst was dispersed in 10 mL solvent, and then added with a required amount of substrate. The autoclave was sealed, purged and pressurized with hydrogen, and then heated to desired temperature under magnetic stirring at a rate of 1000 rpm. After the completion of the reaction, the mixture was separated by centrifugation in order to remove the solid catalyst. The water was removed from the filtrate by evaporation under vacuum in the rotary evaporator at 60 °C. After that, a certain amount of ethanol was added and diluted the mixture to 10 mL. The contents of products and substrate were analyzed by gas-chromatograph (Shimadzu, 2010) with a 30 m capillary column (Rtx[®]-1) using a flame ionization detector (FID). Interpolated calibration was employed for product quantification using standard solutions of substrate and product. All the products were further confirmed by GC-MS (Agilent 6890). The column temperature was raised from 80 to 250 °C with a heating rate of 10 °C/min. The injector temperature was set to 300 °C, which was loaded with a sampling volume of 1 μ L. The conversion of LA and the selectivity of the products (GVL) were calculated according to the following equations:

$$\text{Conversion} = \frac{\text{moles of LA (inlet)} - \text{moles of LA (outlet)}}{\text{moles of LA (inlet)}} \times 100\%$$

$$\text{Selectivity} = \frac{\text{moles of one product}}{\text{moles of all products}} \times 100\%$$

3. Results and discussion

3.1. The structure of catalysts

XRD patterns are shown in Fig. 1. The diffraction pattern of all TiO₂ samples are in good agreement with anatase TiO₂ (JCPDS 21-1272)

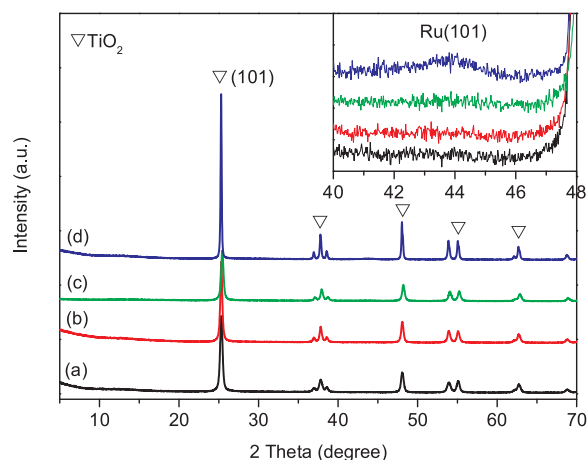


Fig. 1. XRD patterns of (a) Ru/TiO₂-0.4, (b) Ru/TiO₂-1, (c) Ru/TiO₂-2 and (d) Ru/TiO₂-3.

Table 1
Structural properties of nano-TiO₂.

Samples	S _{total} (m ² /g)	Pore volume (cm ³ /g)	Average pore diameter (nm)	TiO ₂ size (nm) ^a	TiO ₂ size (nm) ^b
TiO ₂ -0.4	59.4	0.024	7.37	11.1	34.8 ± 6.6
TiO ₂ -1	48.9	0.018	6.16	11.2	40.6 ± 17.7
TiO ₂ -2	30.8	0.015	7.36	13.6	70.3 ± 27.2
TiO ₂ -3	2.7	0.003	6.44	25.2	385.6 ± 211.9

^a Determined by XRD.

^b Determined by SEM.

[31]. The peak width of (101) diffraction peak becomes sharp as increasing the HF amount from 0.4 to 3.0 mL. The average TiO₂ crystallite sizes of the samples (Table 1) are calculated via the Debye-Scherrer equation based on the main diffraction (101) peak ($2\theta = 25.28^\circ$, Fig. S1), in which the crystallite size of TiO₂-0.4 is around 11.1 nm. UV–vis analysis (Fig. S2) shows that all TiO₂ samples afford similar absorption at wavelength range 200–400 nm. As the HF amount decreases, the absorbance increases gradually, indicating the size of TiO₂ decreases [32]. The morphology of TiO₂ was observed by SEM. As shown in Fig. 2, all samples appear to be composed of primary rough particles and the HF amount has a profound influence in particle size of TiO₂. For example, TiO₂-3 exhibits a big particle size of 385 nm along with a wide size distribution, decreasing the HF amount sharply decreases the particle size as well as size distribution, and TiO₂-0.4 shows particles with fairly uniform size of 34.8 ± 6.6 nm. In addition, with the decrease of the HF amount from 3 to 0.4 mL, the surface areas and pore volumes are largely increased from 2.7 m²/g and 0.003 cm³/g for TiO₂-3 to 59.4 m²/g and 0.024 cm³/g for TiO₂-0.4, respectively (Table 1). These results indicate that the HF amount plays an important role in controlling the particle size of TiO₂ [33].

Ru-based catalysts are synthesized by a facile impregnation strategy using H₂ as the reductant. The XRD pattern (Fig. 1) of Ru/TiO₂-0.4 shows nearly no Ru reflection peak at $2\theta = 44^\circ$ compared with Ru/TiO₂-2 and Ru/TiO₂-3, indicating the presence of small-sized (smaller than 3–4 nm in size) and highly dispersed Ru NPs [34]. TEM images (Fig. 3) reveal that Ru/TiO₂-0.4 is comprised of crystalline TiO₂ NPs of around 30 nm in diameter, well agreed with the SEM images. The HRTEM image (Fig. 3c) shows that Ru NPs with an average size of 1.69 nm are well dispersed in uniform TiO₂ NPs without any aggregation.

In order to further investigate the valence of metal-based species, Ru XPS analyses are measured (Fig. 4). It is found that the Ru 3d spectra of Ru/TiO₂-0.4 exhibits the lowest binding energy in comparison to those of other samples, indicating more intimate interaction occurs between the active Ru sites and TiO₂-0.4, thus leading to electron-sufficient Ru species on TiO₂-0.4 [35].

H₂-TPR profiles of Ru/TiO₂ catalysts are shown in Fig. 5. As for Ru/TiO₂-C derived from commercial TiO₂, a big peak centered at 199 °C with a big shoulder at 173/138 °C can be observed. The reduction peaks of Ru/TiO₂-3 downshift to 148 and 189 °C, indicating the existence of small-sized Ru NPs on surface of TiO₂-3. As for Ru/TiO₂-2, the reduction peak is broad and centers at 169 °C. Further decreasing the HF amount, the reduction peak moves to low-temperature range, and Ru/TiO₂-0.4 affords the lowest reduction temperature (117 and 158 °C), indicating the smallest size of NPs and easiest reduction property of Ru species [34]. It is well known that metals supported on titania exhibit the strong metal-support interaction effect, which leads to the formation of an electron-rich metal [25,36]. Small-sized TiO₂ NPs afford sufficient contact with metal NPs, thus leading to much stronger metal-support interaction, which is known to modify the selectivity and activity of a catalyst [23].

3.2. Hydrogenation of LA over Ru-based catalysts

The hydrogenation of LA to GVL is carried out in water at 30 °C under 1.0 MPa (Table 2). A blank test shows that nearly no LA is transformed when TiO₂-0.4 is used as catalyst (entry 1). Ru/TiO₂-0.4 exhibits significantly higher catalytic activity (97.4%) with a GVL selectivity of 100% (entry 2). Ru/TiO₂-1, Ru/TiO₂-2 and Ru/TiO₂-3 afford 68.2, 62.8 and 15.5% LA conversion, respectively (entries 3–5), much lower than that of Ru/TiO₂-0.4. The TOF value based on total Ru atoms of Ru/TiO₂-0.4 is as high as 799.8 h⁻¹, which is 1.42, 1.54 and 6.26 times of Ru/TiO₂-1, Ru/TiO₂-2 and Ru/TiO₂-3, respectively. For comparative purposes, commercial TiO₂ supported Ru catalyst (Ru/TiO₂-C) shows a poor activity (19.0%) for LA hydrogenation (entry 6). Other frequently used heterogeneous Ru-based catalysts inclusive of Ru/AC, Ru/BC and Ru/MCN achieve obviously slower hydrogenation rate and relatively lower LA conversion (< 50%) under the same conditions (entries 7–9). Some other literatures have also been reported for the low-temperature hydrogenation of LA, but a high hydrogen pressure was generally required [14,20,29]. For example, 4 MPa H₂ was required for the CTH of LA with water over graphene-supported Ru catalysts (Ru/RGO) [20,29]. Obviously, our method is preferable because only 1 MPa and 30 min was needed at room temperature.

The time-on-stream experiments over Ru/TiO₂-0.4 and Ru/TiO₂-3 (Fig. 6) indicate that the hydrogenation rate of LA over Ru/TiO₂-0.4 is much higher than that of Ru/C-TiO₂-3. For example, > 95% conversion was observed in 30 and 150 min for Ru/TiO₂-0.4 and Ru/TiO₂-3, respectively. The catalytic performances of Ru/TiO₂-0.4 were further investigated at lower temperatures (20 and 10 °C) (Table 2, entries 10 and 11). Although an obvious decrease in reaction rate is observed as decreasing the reaction temperature to 20 and 10 °C, Ru/TiO₂-0.4 still gives 99.1 and 88.5% LA conversion by prolonging time to 1.5 and 3 h, respectively, indicating Ru/TiO₂-0.4 is indeed an excellent low-temperature catalyst for LA hydrogenation.

Among the solvents tested (Fig. 7), water is more favorable than organic solvents for LA hydrogenation. Although the solubility of H₂ in water is much lower than in organic solvents, it was reported that H spillover can be greatly promoted by water, and H atom of water participated in the hydrogenation of the C=O group of LA, which enhanced the hydrogenation reaction rate. [37] The reaction slows down at low catalyst loading but without any losing of the selectivity (Fig. 8). The effect of hydrogen pressure on catalytic activity is studied (Fig. 9). Although an obvious decrease in activity is observed as decreasing the hydrogen pressure, Ru/TiO₂-0.4 still gives 33.2% LA conversion at a low hydrogen pressure of 0.2 MPa.

To further showcase the effectiveness of Ru/TiO₂-0.4 catalyst, we carried out the LA hydrogenation on a one-gram scale (Fig. 10). Direct LA (1.16 g) hydrogenation with an even lower catalyst loading of 0.0487 mol% Ru at 30 °C for 10 h provides GVL with 85% yield, which appears to be efficient for industrial application.

To further demonstrate the versatility of the Ru/TiO₂-0.4 catalyst, the selective HDO of biomass-derived vanillin to 2-methoxy-4-methylphenol (MMP) in water was performed at 70 °C under 1.0 MPa H₂ (Table 3). Similarly, Ru/TiO₂-0.4 shows the best activity and affords 53.9% MMP yield for 2 h, this value is 4.6, 6.7 and 8.7 times higher than that of Ru/TiO₂-1, Ru/TiO₂-2 and Ru/TiO₂-3, respectively. Furthermore, nearly 100% conversion and 100% MMP selectivity could reach over Ru/TiO₂-0.4 catalyst by prolonging reaction time to 4 h, along which a high specific activity of 51.3 h⁻¹ could be achieved. The Ru/TiO₂-0.4 catalyst even exhibited much higher activity than other reported metal catalysts [38]. For example, carbon nanotube supported ruthenium catalysts (Ru/CNT) with decalin/H₂O as solvent produced MMP with a slightly lower yield of 93% under harsh conditions (200 °C for 3 h) [38].

Finally, recycling tests are performed to investigate the durability of the catalyst (Fig. 11). The Ru/TiO₂-0.4 shows a good stability with maintained activity and selectivity during the tests. The ICP analysis of

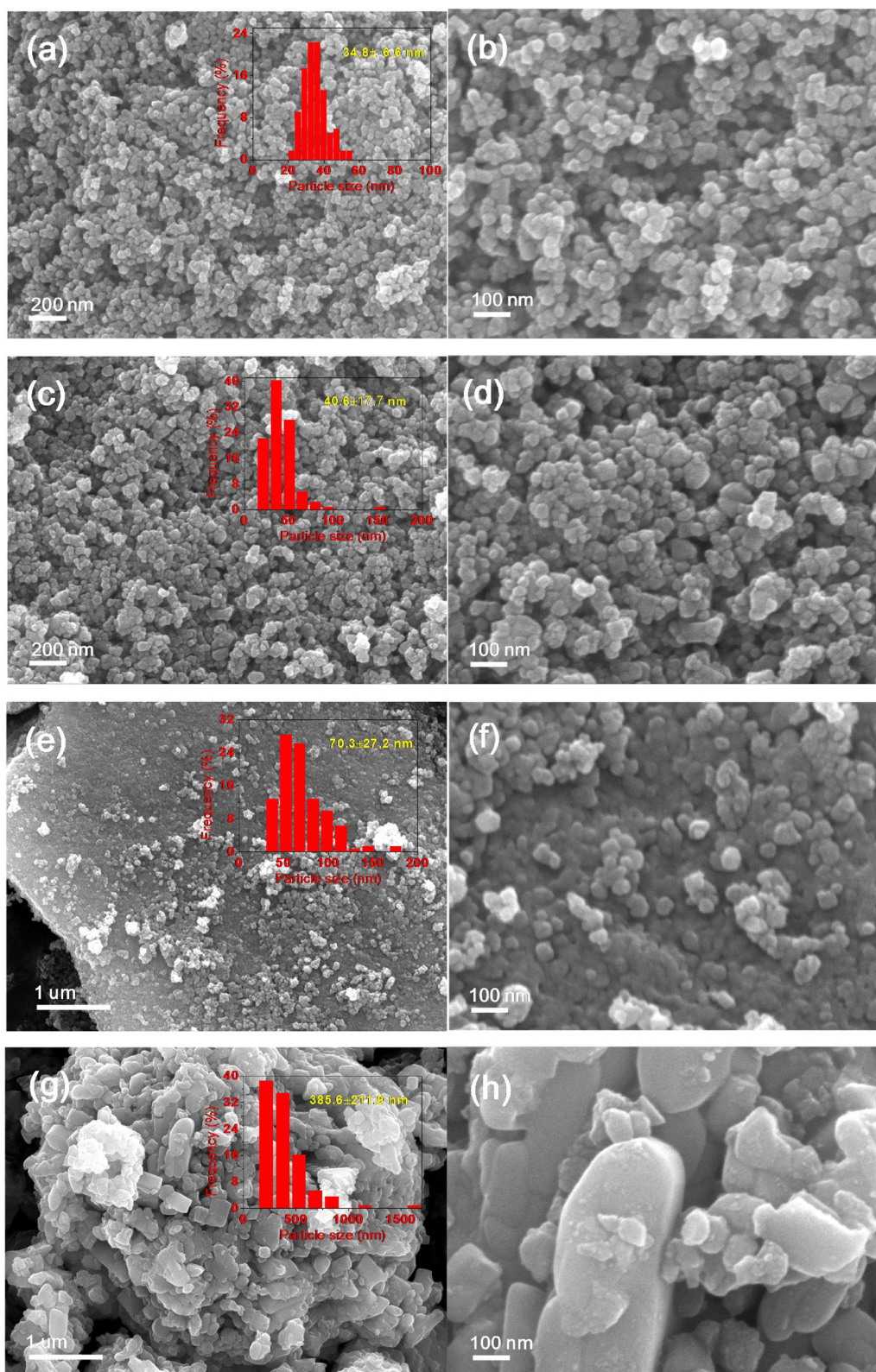


Fig. 2. SEM images of (a, b) Ru/TiO₂-0.4, (c, d) Ru/TiO₂-1, (e, f) Ru/TiO₂-2 and (g, h) Ru/TiO₂-3.

fresh and recovered catalysts reveals no Ru leaching in solution. The dispersion and crystalline state of Ru NPs in recovered catalyst, based on corresponding TEM image (Fig. 12) and XRD pattern (Fig. 13), do not change significantly after five runs, showing a stable nano-structure for highly active Ru NPs toward room-temperature LA hydrogenation in water.

4. Conclusion

The selective hydrogenation of LA to GLV has been studied using uniform-sized TiO₂ supported Ru catalyst (Ru/TiO₂) prepared by an effortless hydrothermal route. The catalytic performance of Ru NPs is affected greatly by the amount of HF that impacts particle size and

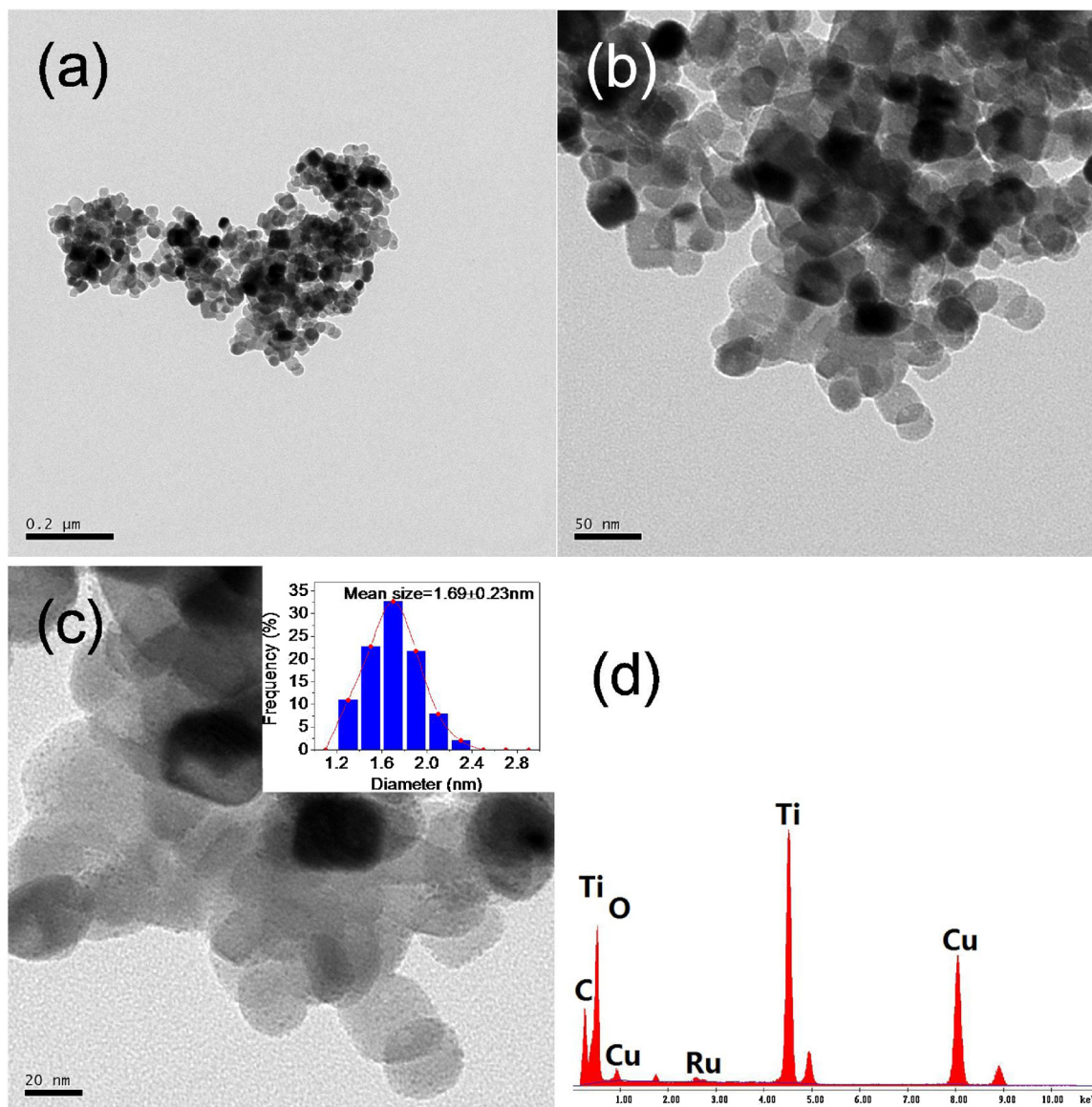


Fig. 3. (a–c)TEM images and (d) EDX analysis of Ru/TiO₂-0.4.

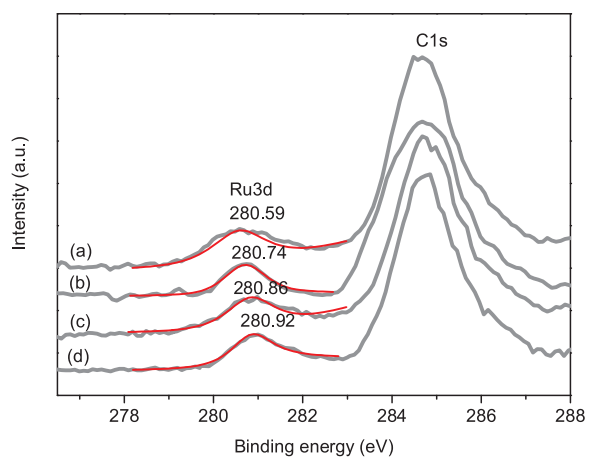


Fig. 4. XPS spectra of Ru 3d of (a) Ru/TiO₂-0.4, (b) Ru/TiO₂-1, (c) Ru/TiO₂-2 and (d) Ru/TiO₂-3.

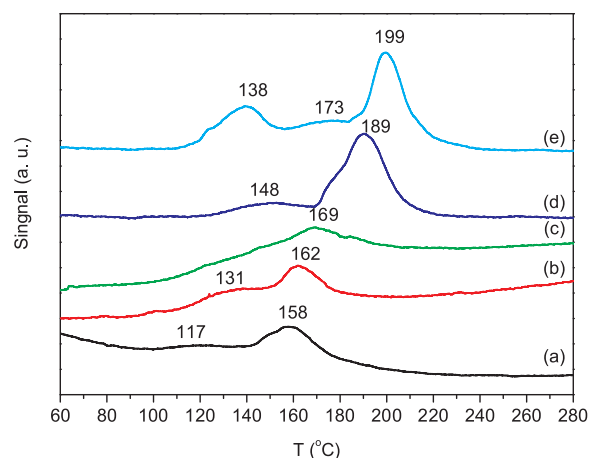


Fig. 5. H₂-TPR spectra of (a) Ru/TiO₂-0.4, (b) Ru/TiO₂-1, (c) Ru/TiO₂-2, (d) Ru/TiO₂-3 and (e) Ru/TiO₂-C.

Table 2
Hydrogenation of LA over different catalysts.^a

Entry	Catalysts	T/°C	t/h	Conversion/%	GLV selectivity/%
1	TiO ₂ -0.4	30	0.5	0.4	–
2	Ru/TiO ₂ -0.4	30	0.5	97.4	> 99
3	Ru/TiO ₂ -1	30	0.5	68.2	> 99
4	Ru/TiO ₂ -2	30	0.5	62.8	> 99
5	Ru/TiO ₂ -3	30	0.5	15.5	> 99
6	Ru/TiO ₂ -C	30	0.5	19.0	> 99
7	Ru/AC	30	0.5	5.8	> 99
8	Ru/BC	30	0.5	46.7	> 99
9	Ru/MCN	30	0.5	33.8	> 99
10	Ru/TiO ₂ -0.4	20	1.5	99.1	> 99
11	Ru/TiO ₂ -0.4	10	3	88.5	> 99

^a Reaction conditions: LA (1 mmol), catalyst (10 mg), H₂O (10 mL), 1.0 MPa H₂.

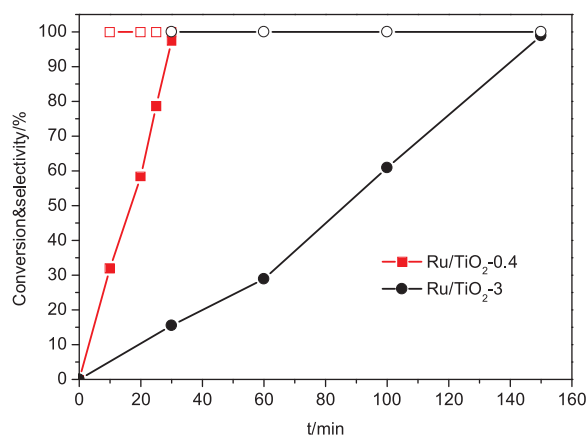


Fig. 6. Selective hydrogenation of LA over Ru/TiO₂-0.4 and Ru/TiO₂-3 catalysts. Reaction conditions: LA (1 mmol), catalyst (10 mg), H₂O (10 mL), 1.0 MPa H₂, 30 °C.

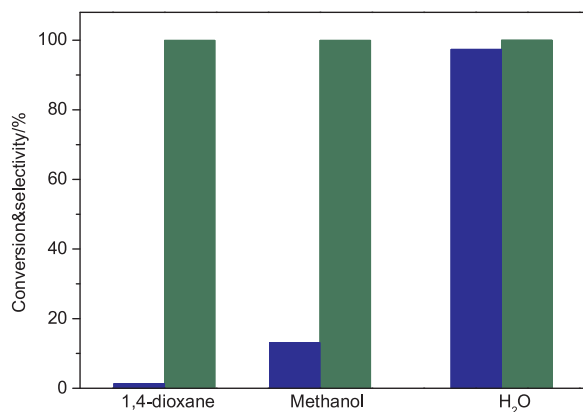


Fig. 7. The effect of solvent on LA hydrogenation. Reaction conditions: LA (1 mmol), Ru/TiO₂-0.4 (10 mg), solvent (10 mL), 1.0 MPa H₂, 30 °C, 0.5 h.

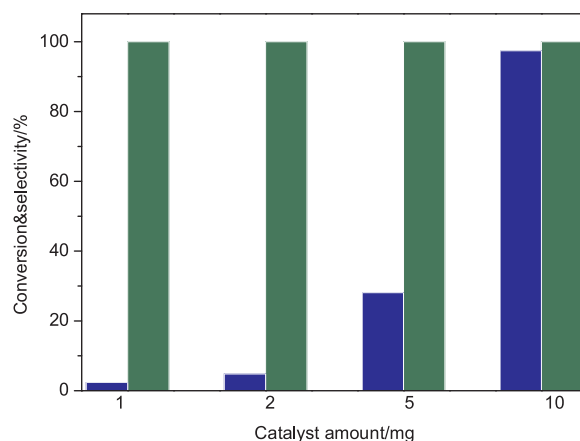


Fig. 8. The effect of catalyst amount on LA hydrogenation. Reaction conditions: LA (1 mmol), Ru/TiO₂-0.4, H₂O (10 mL), 1.0 MPa H₂, 30 °C, 0.5 h.

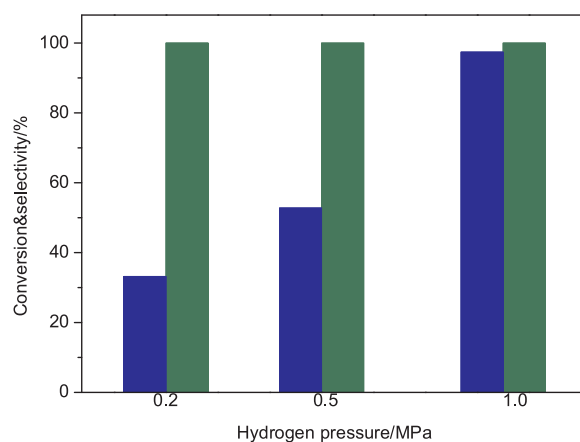


Fig. 9. The effect of hydrogen on LA hydrogenation. Reaction conditions: LA (1 mmol), Ru/TiO₂-0.4 (10 mg), H₂O (10 mL), 30 °C, 0.5 h.

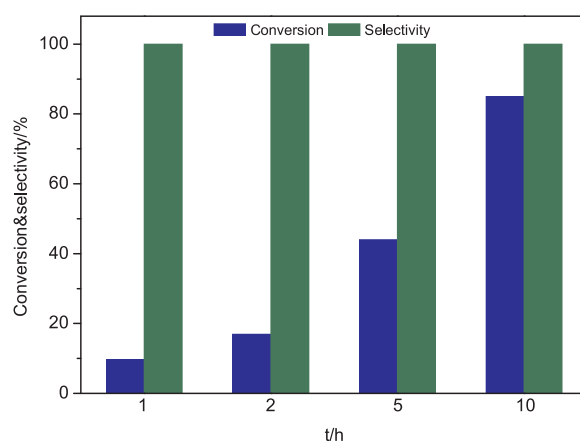
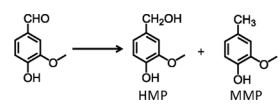


Fig. 10. Gram-scale hydrogenation of LA over Ru/TiO₂-0.4 catalyst. Reaction conditions: LA (10 mmol), catalyst (20 mg), H₂O (40 mL), 3.0 MPa H₂, 30 °C.

Table 3
Hydrogenation of vanillin over different catalysts.^a



Catalyst	t/h	Conversion /%	MMP selectivity/%	MMP Yield/%	TOF/h ^{-1b}
Ru/TiO ₂ -0.4	2	99.3	54.3	53.9	55.3
Ru/TiO ₂ -0.4	4	99.9	99.9	99.9	51.3
Ru/TiO ₂ -1	2	92.5	12.7	11.7	12.1
Ru/TiO ₂ -2	2	87.6	9.3	8.1	8.4
Ru/TiO ₂ -3	2	53.1	11.7	6.2	6.4

^a Reaction conditions: vanillin (0.5 mmol), catalyst (10 mg), H₂O (10 mL), 1.0 MPa H₂, 70 °C.

^b Calculation based on MMP yield.

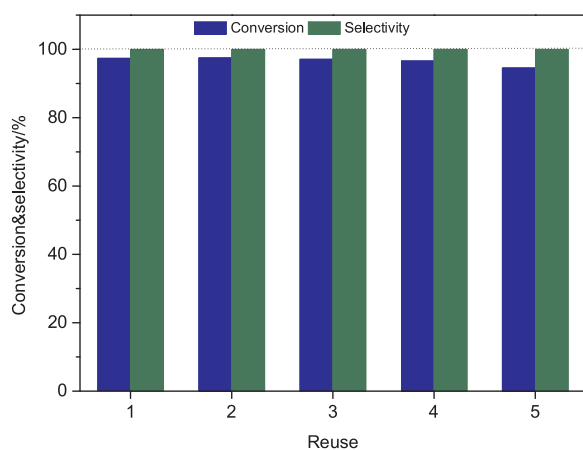


Fig. 11. Re-uses of Ru/TiO₂-0.4 for the selective hydrogenation of LA. Reaction conditions: LA (1 mmol), catalyst (10 mg), H₂O (10 mL), 1.0 MPa H₂, 30 °C, 0.5 h.

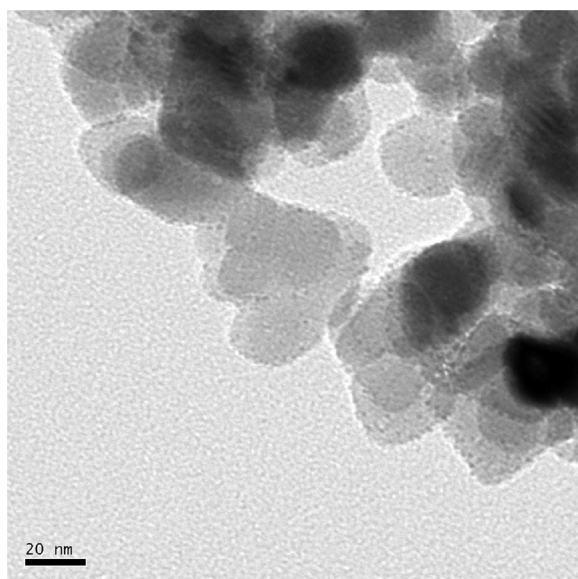


Fig. 12. TEM image of 5-time reused Ru/TiO₂-0.4.

surface area of TiO₂. It is found that Ru/TiO₂-0.4 obtained with 0.4 mL HF amount shows superior catalytic hydrogenation activity as well as high GLV selectivity in water under extremely mild condition (10–30 °C and 0.2–1.0 MPa H₂). This catalyst is stable and versatile for selective

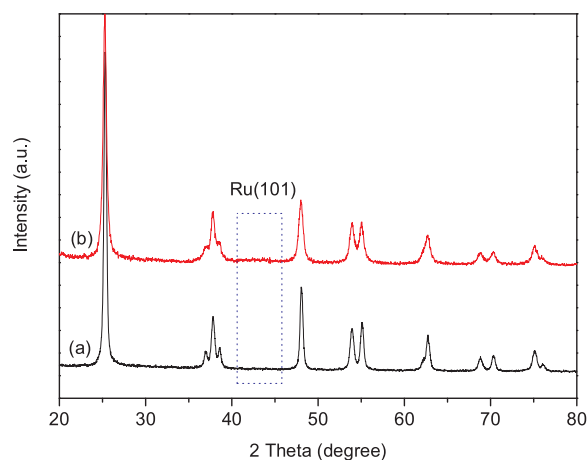


Fig. 13. XRD patterns of (a) fresh and (b) reused Ru/TiO₂-0.4.

HDO of biomass-derived vanillin. XPS and H₂-TPR analyses show that TiO₂-0.4 affords strong electron donation to Ru NPs and easier reducibility of Ru species due to its smaller nanosize, thus boosting Ru for selective transformation of substrates.

Acknowledgements

This work was supported by National Natural Science Foundation of China (21603066, 21606075, 21708006), Natural Science Fund of Hubei Province (2015CFB232) and Natural Science Fund of the Education Department of Hubei Province (Q2015009).

Appendix A. Supplementary data

Supplementary data associated with this article can be found, in the online version, at <http://dx.doi.org/10.1016/j.mcat.2018.05.030>.

References

- [1] R.M. Navarro, M.A. Peña, J.L.G. Fierro, *Chem. Rev.* 107 (2007) 3952–3991.
- [2] P. Gallezot, *Chem. Soc. Rev.* 41 (2012) 1538–1558.
- [3] H. Mehdi, V. Fabos, R. Tuba, A. Bodor, L.T. Mika, I.T. Horvath, *Top. Catal.* 48 (2008) 49–54.
- [4] W.R.H. Wright, R. Palkovits, *ChemSusChem* 5 (2012) 1657–1667.
- [5] A.M. Hengne, C.V. Rode, *Green Chem.* 14 (2012) 1064–1072.
- [6] W. Hao, W. Li, X. Tang, X. Zeng, Y. Sun, S. Liu, L. Lin, *Green Chem.* 18 (2016) 1080–1088.
- [7] K.-i. Shimizu, S. Kanno, K. Kon, *Green Chem.* 16 (2014) 3899–3903.
- [8] A.M. Ruppert, J. Grams, M. Jędrzejczyk, J. Matras-Michalska, N. Keller, K. Ostojaska, P. Sautet, *ChemSusChem* 8 (2015) 1538–1547.
- [9] K. Jiang, D. Sheng, Z. Zhang, J. Fu, Z. Hou, X. Lu, *Catal. Today* 274 (2016) 55–59.
- [10] X. Long, P. Sun, Z. Li, R. Lang, C. Xia, F. Li, *Chin. J. Catal.* 36 (2015) 1512–1518.
- [11] J. Lv, Z. Rong, Y. Wang, J. Xiu, Y. Wang, J. Qu, *RSC Adv.* 5 (2015) 72037–72045.
- [12] W. Luo, M. Sankar, A.M. Beale, Q. He, C.J. Kiely, P.C.A. Bruijninx, B.M. Weckhuysen, *Nat. Commun.* 6 (2015) 6540.
- [13] J. Ftouni, A. Muñoz-Murillo, A. Goryachev, J.P. Hofmann, E.J.M. Hensen, L. Lu, C.J. Kiely, P.C.A. Bruijninx, B.M. Weckhuysen, *ACS Catal.* 6 (2016) 5462–5472.
- [14] C. Xiao, T.-W. Goh, Z. Qi, S. Goes, K. Brashler, C. Perez, W. Huang, *ACS Catal.* 6 (2015) 593–599.
- [15] W. Li, J.-H. Xie, H. Lin, Q.-L. Zhou, *Green Chem.* 14 (2012) 2388–2390.
- [16] S.G. Wettstein, J.Q. Bond, D.M. Alonso, H.N. Pham, A.K. Datye, J.A. Dumesic, *Appl. Catal. B* 117–118 (2012) 321–329.
- [17] Y. Yang, G. Gao, X. Zhang, F. Li, *ACS Catal.* 4 (2014) 1419–1425.
- [18] A.M. Ruppert, M. Jędrzejczyk, O. Sneka-Platek, N. Keller, A.S. Dumon, C. Michel, P. Sautet, J. Grams, *Green Chem.* 18 (2016) 2014–2028.
- [19] M. Sudhakar, M. Lakshmi Kantam, V. Swarna Jaya, R. Kishore, K.V. Ramanujachary, A. Venugopal, *Catal. Commun.* 50 (2014) 101–104.
- [20] J. Tan, J. Cui, G. Ding, T. Deng, Y. Zhu, Y.-W. Li, *Catal. Sci. Technol.* 6 (2016) 1469–1475.
- [21] J.-P. Lange, R. Price, P.M. Ayoub, J. Louis, L. Petrus, L. Clarke, H. Gosselink, *Angew. Chem. Int. Ed.* 49 (2010) 4479–4483.
- [22] X. Kong, Y. Zhu, H. Zheng, X. Li, Y. Zhu, Y.-W. Li, *ACS Catal.* 5 (2015) 5914–5920.
- [23] M. Shekhar, J. Wang, W.-S. Lee, W.D. Williams, S.M. Kim, E.A. Stach, J.T. Miller, W.N. Delgass, F.H. Ribeiro, *J. Am. Chem. Soc.* 134 (2012) 4700–4708.
- [24] R. Nie, H. Jiang, X. Lu, D. Zhou, Q. Xia, *Catal. Sci. Technol.* 6 (2016) 1913–1920.
- [25] K.V. Kovtunov, D.A. Barskiy, O.G. Salnikov, D.B. Burueva, A.K. Khudorozhkov, A.V. Bukhtiyarov, I.P. Prosvirin, E.Y. Gerasimov, V.I. Bukhtiyarov, I.V. Koptuyug,

- ChemCatChem 7 (2015) 2581–2584.
- [26] R. Nie, H. Yang, H. Zhang, X. Yu, X. Lu, D. Zhou, Q. Xia, *Green Chem.* 19 (2017) 3126–3134.
- [27] R. Nie, J. Wang, L. Wang, Y. Qin, P. Chen, Z. Hou, *Carbon* 50 (2012) 586–596.
- [28] R. Nie, M. Miao, W. Du, J. Shi, Y. Liu, Z. Hou, *Appl. Catal. B* 180 (2016) 607–613.
- [29] J. Tan, J. Cui, X. Cui, T. Deng, X. Li, Y. Zhu, Y. Li, *ACS Catal.* 5 (2015) 7379–7384.
- [30] S.W. Hummers, R.E. Offeman, *J. Am. Chem. Soc.* 80 (1958) 1339.
- [31] H. Xu, S. Ouyang, P. Li, T. Kako, J. Ye, *ACS Appl. Mater. Interfaces* 5 (2013) 1348–1354.
- [32] G. Liu, C. Sun, H.G. Yang, S.C. Smith, L. Wang, G.Q. Lu, H.-M. Cheng, *Chem. Commun.* 46 (2010) 755–757.
- [33] J.S. Chen, X.W. Lou, *Electrochem. Commun.* 11 (2009) 2332–2335.
- [34] X. Yu, R. Nie, H. Zhang, X. Lu, D. Zhou, Q. Xia, *Microporous Mesoporous Mater.* 256 (2018) 10–17.
- [35] L. Wang, B. Zhang, X. Meng, D.S. Su, F.-S. Xiao, *ChemSusChem* 7 (2014) 1537–1541.
- [36] S. Sakellson, M. McMillan, G.L. Haller, *J. Phys. Chem.* 90 (1986) 1733–1736.
- [37] J. Tan, J. Cui, T. Deng, X. Cui, G. Ding, Y. Zhu, Y. Li, *ChemCatChem* 7 (2015) 508–512.
- [38] X. Yang, Y. Liang, Y. Cheng, W. Song, X. Wang, Z. Wang, J. Qiu, *Catal. Commun.* 47 (2014) 28–31.